Biophysical Chemistry 158 (2011) 150–156

Contents lists available at ScienceDirect

Biophysical Chemistry

journal homepage: http://www.elsevier.com/locate/biophyschem

Structural characterization of liposomes made of diether archaeal lipids and dipalmitoyl-L-α-phosphatidylcholine

Dejan Gmajner [a], Pegi Ahlin Grabnar [b], Magda Tušek Žnidarič [a], Jasna Štrus [a], Marjeta Šentjurc [c], Nataša Poklar Ulrih [a,d,*]

[a] Biotechnical Faculty, University of Ljubljana, Ljubljana, Slovenia
[b] Faculty of Pharmacy, University of Ljubljana, Ljubljana, Slovenia
[c] Jožef Stefan Institute, Ljubljana, Slovenia
[d] CipKeBiP, The Centre of Excellence for Integrated Approaches in Chemistry and Biology of Proteins, Jamova 39, Ljubljana, Slovenia

ARTICLE INFO

Article history:
Received 24 May 2011
Received in revised form 21 June 2011
Accepted 21 June 2011
Available online 30 June 2011

Keywords:
Archaeosome
Lipid mixture
Electron paramagnetic resonance
Fluorescence anisotropy
Photon correlation spectroscopy
Transmission electron microscopy

ABSTRACT

The physicochemical properties of binary lipid mixtures of diether $C_{25,25}$ lipids and dipalmitoyl-L-α-phosphatidylcholine (DPPC) were studied using photon correlation, fluorescence and electron paramagnetic resonance spectroscopy, and transmission electron microscopy. These two types of lipids can be mixed at all molar ratios to form unilamellar and multilamellar liposomes. Fluorescence anisotropy of 1,6-diphenyl-1,3,5-hexatrien in mixed liposomes indicates that the abrupt changes in order parameter in the hydrophobic part of bilayer membranes made of DPPC lipids disappears with increasing mol% $C_{25,25}$ lipids. Electron paramagnetic resonance spectroscopy shows that at temperatures below 50 °C, the interfacial regions of membrane bilayer of mixed liposomes is more fluid than for pure DPPC liposomes, while at higher temperatures, the impact of the long isoprenoid chains on the membrane stability becomes more pronounced. Photon correlation spectroscopy and transmission electron microscopy show that mixed liposomes do not fuse or aggregate, even after 41 days at 4 °C.

1. Introduction

The molecular adaptations that promote the ability of archaea to survive and grow in harsh environments have clearly emphasized the key role of membrane lipid components. These can help to overcome the destabilizing conditions that are encountered in such extreme environments as hot acidic springs and sub-marine volcanic fields. Polar archaeal lipids are generally composed of a core lipid and a phosphodiester-bonded polar head group or glycoside that is linked to one of the core lipids. The cell membrane of the hyperthermophilic archaeon *Aeropyrum pernix* K1 is comprised of only two major polar lipids. The core lipid consists solely of $C_{25,25}$-archaeol (2,3-di-sesterpanyl-*sn*-glycerol). C_{25-25}-archaetidyl(glucosyl)inositol (AGI), with its glucosylinositol polar head group accounts for 91 mol%, with $C_{25,25}$-archaetidylinositol (AI) with its myoinositol polar head group, accounts for 9 mol% [1]. The lipids of *A. pernix* are different from those of the anaerobic sulfur-dependent hyperthermophiles (e.g. *Sulfolobus solfataricus*) [2,3] in terms of a lack of tetraether lipids and a direct linkage of inositol and sugar moieties. Unlike the tetraether lipids, which can form simple monolayers due to their bipolarity, monopolar $C_{25,25}$ lipids form bilayers. The unique structures and properties of bipolar tetraether lipids have been extensively studied [4,5]. However, it has been shown that the cell membrane of *A. pernix* and liposomes prepared solely from these $C_{25,25}$ lipids, known as archaeosomes, have some unique properties [6,7]. We have shown that archeosomes made of $C_{25,25}$ lipids do not show the typical gel-to-liquid crystalline transition in the temperature range from 0 °C to 100 °C, and that they are stable in a pH range from 4 to 12. Additionally, our data have indicated that archaeosomes in the pH range from 4 to 12 release less than 27% of entrapped calcein after during incubation for 10 h at 90 °C. Fluorescence anisotropy with the hydrophobic probe 1,6-diphenyl-1,3,5-hexatriene (DPH) have shown only gradual changes in order parameter of these membranes up to 60 °C. From the electron paramagnetic resonance (EPR) spectr spectra, the mean membrane fluidity that is determined according to maximal hyperfine splitting and empirical correlation times shows a continuous increase with temperature. Above 65 °C, the presence of only fluid-like domains was detected.

Very recently, we showed that even 5 mol% $C_{25,25}$ lipids in mixed $C_{25,25}$-dipalmitoyl-L-α-phosphatidylcholine (DPPC) liposomes

Abbreviations: AGI, C_{25-25}-archaetidyl(glucosyl)inositol; AI, $C_{25,25}$-archaetidylinositol; DPH, 1,6-diphenyl-1,3,5-hexatriene; DPPC, dipalmitoyl-L-α-phosphatidylcholine; DSC, differential scanning calorimetry; EPR, electron paramagnetic resonance; HEPES, 4-(2-hydroxyethyl)-1-piperazineethanesulfonic acid; LUVs, large unilamellar vesicles; MeFASL(10,3), methylester of 5-doxyl palmitic acid; MLVs, multilamellar vesicles; PCS, photon correlation spectroscopy; PI, polydispersity index; SUVs, small unilamellar vesicles; TEM, transmission electron microscopy.

* Corresponding author at: University of Ljubljana, Biotechnical Faculty, Jamnikarjeva 101, 1000 Ljubljana, Slovenia. Tel.: +386 1 3230780; fax: +386 1 2566296.
E-mail address: natasa.poklar@bf.uni-lj.si (N.P. Ulrih).

0301-4622/$ – see front matter © 2011 Elsevier B.V. All rights reserved.
doi:10.1016/j.bpc.2011.06.014

drastically influences the phase transition of liposomes. However, the low content of $C_{25,25}$ lipids in these mixed liposomes stabilizes them against releasing entrapped calcein at temperatures above the phase transition of DPPC [8]. As a continuation of our previous studies in the field of archaeal diether lipids, we present here the structural properties of liposomes prepared from binary lipid mixtures of diether $C_{25,25}$ lipids and DPPC.

To date, several successful archaeal lipid mixtures with conventional lipids have been characterized by various techniques, such as those with egg phosphatidylcholine [9,10], These techniques have involved fluorescence polarization and anisotropy, calcein release and proton permeation, differential scanning calorimetry (DSC), and more recently, also small-angle neutron scattering, small-angle X-ray scattering [5,11], nuclear magnetic resonance [12] and pressure perturbation calorimetry [13]. Priming the synthetic phospholipids with tetraether lipids result in the creation of a thermostable membrane, which can be used for stabilization of bicelles, worm-like micelles, and perforated lamellae [11].

2. Experimental procedures

2.1. Growth of A. pernix K1

The optimum conditions for maximizing *A. pernix* biomass were obtained when $Na_2S_2O_3 \times 5H_2O$ (1 g of per liter) (Alkaloid, Skopje, Macedonia) added Marine Broth 2216 (Difco™, Becton, Dickinson and Co., Sparks, USA) at pH 7.0 (20 mM HEPES buffer) was used as a growing medium in 1 L flask at 92 °C (for details see [14]). After growth, the cells were harvested by centrifugation, washed and lyophilized.

2.2. Isolation and purification of lipids, and vesicle preparation

The polar lipid methanol fraction composed of approximately 91% AGI and 9% AI [1] (average molecular mass, 1181.42 g mol^{-1}) was purified from lyophilized *A. pernix* cells, as described previously [7]. After isolation, the lipids were fractionated with adsorption chromatography [15], and the polar lipid methanol fraction was used for further analysis. Organic solvents were removed under a stream of dry nitrogen, followed by the removal of the last traces under vacuum. For mixed lipid liposomes, the appropriate mass of $C_{25,25}$ lipids and DPPC were dissolved in chloroform and mixed together in glass round-bottomed flasks. The lipid film was prepared by drying the sample on a rotary evaporator. For preparation of a pure DPPC lipid film, chloroform/ methanol (7/3, v/v) was used as solvent. The dried lipid films were then hydrated either with warm (~45 °C) 20 mM HEPES buffer, pH 7.0, for fluorescence and EPR spectroscopy, or with deionized water (MilliQ) for transmission electron microscopy (TEM) and photon correlation spectroscopy (PCS) measurements. The mol% of the diether $C_{25,25}$ lipids in the mixed $C_{25,25}$-DPPC liposomes was: 100 (pure $C_{25,25}$), 75, 50, 25 and 0 (pure DPPC). Multilamellar vesicles (MLVs) were prepared by vortexing the lipid suspensions vigorously for 10 min. MLVs were further transformed into small unilamellar vesicles (SUVs) by 30 min sonication, with 10-s on-off cycles at 50% amplitude with a Vibracell Ultrasonic Disintegrator VCX 750 (Sonics and Materials, Newtown, USA). Large unilamellar vesicles (LUVs) were also prepared from MLVs. After six freeze (liquid nitrogen) and thaw (warm water) cycles, the liposomes were pressure-extruded 21 times through 100-nm polycarbonate membranes on an Avanti polar mini-extruder (Avanti Polar Lipids, Alabaster, Alabama, USA), at between 50 °C and 60 °C. Vesicles filled with calcein were prepared by hydrating the dry lipid film with 80 mM calcein (Sigma-Aldrich Chemie GmbH, Steinheim, Germany) in 20 mM HEPES buffer, pH 7.0, for SUVs and LUVs prepared as described above. Gel filtration on Sephadex G-50 (Pharmacia Fine Chemicals AB, Uppsala, Sweden) columns was used to remove extra-vesicular calcein.

2.3. Size distribution and zeta potential analysis

The size distribution and zeta potential of mixed $C_{25,25}$-DPPC SUVs, LUVs and MLVs with different mol% $C_{25,25}$ lipids (100, 75, 50, 25, 0) were determined immediately after their preparation (day 0), and after 13 days (day 13) and 41 days (day 41).

Size measurements of the samples were performed at 25 °C by PCS on a Zetasizer Nano ZS (Malvern Instruments Ltd, Malvern, UK), which used a 4 mW He-Ne laser operating at a wavelength of 633 nm and a detection angle of 173°. A viscosity of 0.8872 mPa s and a refractive index of 1.33 were used for the deionised water at 25 °C in all of these measurements. The data are given as the z-average diameter (intensity-weighted diameter, assuming spherical particles) and the polydispersity index (PI; as a measure of the relative width of the particle size distribution). The surface charge of the liposomes was quantified as the zeta potential by laser Doppler velocimetry using a Zetasizer Nano ZS (Malvern Instruments Ltd, Malvern, UK). The measurements were performed in a folded capillary cell (DTS 1060 C, Malvern Instruments). The zeta potentials were calculated from the electrophoretic mobility by applying the Smoluchowski equation.

2.4. Transmission electron microscopy

Mixed liposomes of $C_{25,25}$-DPPC consisting of different mol% $C_{25,25}$ lipids (100, 75, 50, 25, 0) were examined under TEM (Philips CM 100; Amsterdam, The Netherlands) using the negative-staining method. Twenty microliter liposome suspensions were applied to Formvar-coated and carbone-stabilized copper grids and stained with 2.5% aqueous solution of ammonium molybdate. The morphologies of freshly prepared SUVs, LUVs and MLVs, and those after 41 days of storage under a nitrogen atmosphere at 4 °C, were examined with TEM, operating at 80 kV, and the images were recorded with a Bioscan CCD camera using Digital Micrograph Software (Gatan Inc., Washington, USA).

2.5. Fluorescence anisotropy measurements

Fluorescence anisotropy of DPH (Sigma-Aldric Chemie GmbH, Steinheim, Germany) in mixed $C_{25,25}$-DPPC SUVs consisting of 100, 75, 50, 25 and 0 mol% $C_{25,25}$ lipids was performed in 10-mm-path-length cuvettes using a Cary Eclipse fluorescence spectrophotometer (Varian, Mulgrave, Australia). The measurements were performed over a temperature range of 10 °C to 98 °C at pH 7.0, using Varian auto polarizers with slit widths with a nominal band-pass of 5 nm for both excitation and emission. The DPH was dissolved in dimethyl sulfoxide (Merck KGaA, Darmstadt, Germany) at a concentration of 130 μM. Ten microliter of this DPH solution was added to 2.5 ml of 100 μM SUVs in 20 mM HEPES, to give a final DPH concentration of 0.5 μM. DPH fluorescence anisotropy was measured at an excitation wavelength of 358 nm with the excitation polarizer oriented in the vertical position, with a monocromator at 410 nm used to record the vertical and horizontal components of polarized emission light. The emission fluorescence intensity of DPH in aqueous solution is negligible. The anisotropy (r) was calculated using the built-in software of the instrument (Eq. (1)):

$$r = \frac{I_{||} - I_{\perp}}{I_{||} + 2I_{\perp}} \tag{1}$$

where I_{II} and I are the parallel and perpendicular emission intensities, respectively. Lipid order parameter, S, was calculated from the anisotropy by the following analytical expression [16]:

$$S = \frac{\left[1 - 2(r/r_0) + 5(r/r_0)^2\right]^{1/2} - 1 + r/r_0}{2(r/r_0)} \tag{2}$$

where r_0 is the fluorescence anisotropy value of DPH in the absence of any rotational motion of the probe. The theoretical value of r_0 is 0.4, while experimental values of r_0 lie between 0.362 and 0.394 [16].

2.6. Electron paramagnetic resonance

For EPR measurements, mixed $C_{25,25}$-DPPC SUVs containing different mol%$C_{25,25}$ lipids (100, 75, 50, 25, 0) were spin labeled with a methylester of 5-doxyl palmitic acid (MeFASL(10,3)), which was selected due to its high lipophilicity and its relatively high resolution abilities for local membrane ordering and dynamics. This spin probe exhibit nitroxide moiety at the 5th C atom of the alkyl chain (counting from the methyl group) and therefore monitors characteristics of the more superficial regions of both monolayers forming the membrane bilayer, and not the fatty acid core. A MeFASL (10,3) film was dried onto the wall of a glass tube, and 50 μl of 10 mg ml^{-1} lipid samples in 20 mM HEPES buffer, pH 7.0, was added. The samples were then vortexed for 15 min, giving a final molar ratio of MeFASL(10,3):lipids of 1:250. The EPR spectra of SUVs were recorded with a Bruker ESP 300 X-band spectrometer (Bruker Analytishe Messtechnik, Rheinstein, Germany) using the following parameters: center field, 332 mT; scan range, 10 mT; microwave power, 20.05 mW; microwave frequency, 9.32 GHz; modulation frequency, 100 kHz; modulation amplitude, 0.2 mT; temperature range; 5 °C to 95 °C. Each spectrum was the average of 10 scans, in order to improve the signal-to-noise ratio. The mean empirical correlation time (τ_{emp}) was calculated from the EPR spectra using Eq. (3)[17].

$$\tau_{emp} = k\Delta Ho[(h_0/h_{-1})^{\frac{1}{2}} - 1] \quad (3)$$

The line width (ΔH_0) in mT and the height of the mid-field (h_0) and high-field (h_{-1}) lines were obtained from the EPR spectra [17]; k is a constant typical for the spin probe; 5.9387×10^{-11} mT^{-1} for MeFASL(10,3).

2.7. Computer simulation of electron paramagnetic resonance spectra

For more precise descriptions of the membrane characteristics, computer simulations of the EPR spectra line shapes were performed using the EPRSIM program (Janez Štrancar, 1996–2003, http://www2.ijs.si/~jstrancar/software.htm) and this has been described in more details elsewhere [18]. The model takes into account the membrane characteristics, as heterogeneous, and composed of several coexisting domains with different fluidity characteristics. Therefore, the EPR spectrum is composed of several spectral components that reflect different modes of restricted rotational motion of the spin-probe molecules in different membrane environments. Each spectral component is described with a set of spectral parameters, which define the line shape. These are: order parameter (S), rotational correlation time (τ_c), and line width correction (W) and polarity correction of the magnetic tensors g and A (p_g and p_A, respectively). The order parameter describes the orientation order of the alkyl chains of the phospholipids in the membrane domains, with $S=1$ for perfectly ordered chains, and $S=0$ for isotropic alignment of the chains. More fluid membrane domains are characterized by a small S. The rotational correlation time (τ_c) describes the dynamics of the spin-probe motion, the line width correction (W) is due to the unresolved hydrogen super-hyperfine interactions and contributions from other paramagnetic impurities (e.g., oxygen, external magnetic field inhomogeneities), and the polarity correction arises from the polarity of the spin-probe nitroxide group environment. Besides these parameters, the line shape of the EPR spectra is defined by the relative proportion of each spectral component (d), which describes the relative amount of spin probes with particular motional modes, and depends on the distribution of the spin probe between the coexisting domains with different fluidity characteristics. As the partitioning of MeFASL(10,3) has been shown to be approximately equal between the different domain types of phospholipid/cholesterol vesicles [19], we assumed that the same is valid also for diether $C_{25,25}$ liposomes. It should be stressed that the lateral motion of the spin probe is slow on the time scale of the EPR spectra [20]. Therefore, an EPR spectrum describes only the properties of the nearest surroundings of a spin probe, on the nm scale. All of the regions in the membrane with similar modes of spin-probe motion contribute to one and the same spectral component. Thus, each spectral component reflects the fluidity characteristics of a certain type of membrane domain (with dimensions of several nm) [21]. To obtain the best fit of a calculated EPR spectrum to the experimental one, the multi-run hybrid evolutionary optimization algorithm is used [21], together with a newly developed GHOST condensation procedure [22].

3. Results and discussion

3.1. Mean diameter and zeta potential of liposomes

The mean diameters, polydispersity indices and zeta potentials of pure $C_{25,25}$ archaeosomes, mixed $C_{25,25}$-DPPC liposomes (at the different ratios) and pure DPPC liposomes prepared by the three methods are presented in Table 1. The mean diameter of MLVs formed with 100 mol% DPPC is in the micrometer range (3 μm). With increasing mol%$C_{25,25}$ lipids in the mixed $C_{25,25}$-DPPC liposomes, their mean diameters decreased, and at 50 mol% and 75 mol%$C_{25,25}$ lipids they were 530 ± 370 nm to 570 ± 370 nm, which is also the size of pure $C_{25,25}$ liposomes. The polydispersity index of all of the MLV samples was lower than 0.5. The incorporation of $C_{25,25}$ lipids into the lipid bilayer has an influence on zeta potential: with an increasing portion of $C_{25,25}$ lipids in binary mixtures, the zeta potential decreased from -7 ± 20 mV for 100 mol% DPPC to -94 ± 15 mV for 100 mol%$C_{25,25}$ lipids . The mean diameter of the LUVs (prepared by extrusion) and SUVs (prepared by sonication) of 100 mol% DPPC were 190 ± 120 nm and 75 ± 30 nm, respectively. The LUVs and SUVs containing 25 mol%$C_{25,25}$ lipids were smaller (110 ± 25 nm and 40 ± 25 nm, respectively). With further increases in the mol%$C_{25,25}$ lipids in binary mixtures, no significant decreases in the size and zeta potential of the liposomes was observed. From the data presented in Table 1, we can conclude that $C_{25,25}$ lipids at all mol ratios in mixed $C_{25,25}$-DPPC liposomes (as LUVs and SUVs) are likely to form liposomes with a uniform size distribution and surface charge (zeta potential -50 mV to -60 mV). The incorporation of the negatively charged $C_{25,25}$ lipids into the zwitterionic DPPC liposomes decreased

Table 1
Characteristics of the mixed $C_{25,25}$-DPPC MLVs, LUVs and SUVs composed of different mol%$C_{25,25}$ lipids.

Liposome type	$C_{25,25}$ lipids (mol%)	Mean diameter (nm)	Polydispersity index	Zeta potential (mV)
MLV	0	3000 ± 1200	0.16	-7 ± 20
	25	850 ± 420	0.24	-76 ± 10
	50	570 ± 300	0.26	-92 ± 15
	75	530 ± 370	0.49	-92 ± 13
	100	540 ± 340	0.40	-94 ± 15
LUV	0	190 ± 120	0.43	-1 ± 6
	25	110 ± 25	0.05	-52 ± 14
	50	110 ± 30	0.09	-60 ± 14
	75	110 ± 30	0.08	-60 ± 12
	100	115 ± 30	0.08	-63 ± 11
SUV	0	75 ± 30	0.17	-5 ± 8
	25	40 ± 25	0.24	-55 ± 11
	50	60 ± 35	0.34	-60 ± 15
	75	40 ± 20	0.28	-53 ± 19
	100	60 ± 30	0.25	-50 ± 20

the size and increased the physical stability of the dispersion. As can be seen from Fig. 1, the mean diameters and zeta potentials of the MLVs, SUVs and LUVs prepared from these $C_{25,25}$-DPPC mixtures did not change significantly, even after six weeks of storage at 4 °C (Fig. 1).

3.2. Transmission electron microscopy

Representative TEM micrographs of pure $C_{25,25}$ lipids, DPPC lipids, and mixed MLVs, LUVs and SUVs of $C_{25,25}$-DPPC lipids at different molar ratios are shown in Fig. 2. TEM observation using ammonium molybdate for negative staining showed the vesicle shapes and sizes, and also obtained good contrast for information relating to their structure, like the presence of multilamellarity. Pure DPPC MLVs had a high level of multilamellarity demonstrating also the coalescence and/or fusion; it was almost impossible to differentiate between individual liposomes. In the presence of the $C_{25,25}$ lipids, a large change in the morphology of the MLVs was seen: the liposomes were smaller and less multilamellar. The degree of coalescence/fusion here depended on the mol% of the $C_{25,25}$ lipids in the mixture, while in the pure archaeal liposomes (A100) there was almost no fusion seen. These vesicles were clearly separated, and they had irregular shapes. These observations were consistent with the PCS measurements (Table 1). For pure DPPC LUVs prepared by extrusion, larger sizes and higher PIs were seen in comparison with the mixed $C_{25,25}$-DPPC LUVs (Fig. 1). While the mixed $C_{25,25}$-DPPC liposomes with 25 mol% $C_{25,25}$ lipids (Fig. 2, A25) appeared to have similar images as those made of DPPC, TEM micrographs of the other two mixtures of 50 mol% and 75 mol% $C_{25,25}$ lipids (A50 and A75) and the pure $C_{25,25}$ lipids showed equal size and shape distributions. In comparison to equimolar LUVs, SUVs formed slightly smaller and less uniformly sized vesicles (Table 1). With the LUVs and SUVs, no multillamelarity was observed, regardless of the mol% $C_{25,25}$ lipids in the mixed $C_{25,25}$-DPPC liposomes (Fig. 2). In pure $C_{25,25}$ SUVs, some fusion occurred, which is likely to lead to formation of membrane structures (data not shown) rather than to formation of MLVs.

3.3. Fluorescence anisotropy measurements

Steady-state anisotropy measurements of DPH were performed to compare the levels of order in the $C_{25,25}$-DPPC mixed liposomes, by changing the content of diether lipids. In general, with respect to the lipid bilayer structures, the anisotropy values were highest in the gel state, lowest in the liquid-disordered state, and intermediate in the liquid-ordered state [23]. The lipid order paramereters were calculated by using Eq. (2) from anisotropy measurements of DPH in the $C_{25,25}$-DPPC mixed liposomes at different temperatures (Fig. 3). The order parameter in pure diether $C_{25,25}$ archaeosomes decreased gradually with increasing temperature (Fig. 3). The initial order parameter values of DPH in pure $C_{25,25}$ lipids and in pure DPPC lipids at 10 °C and pH 7.0 were 0.883 ± 0.009 and 0.971 ± 0.009, respectively [7]. Under these conditions, the DPPC lipids are in a gel-crystalline state. The mixed liposomes of different mol% $C_{25,25}$ lipids and DPPC had order parameter values between pure $C_{25,25}$ lipids and DPPC lipids (Fig. 3). Similar behavior was also observed by Lelkes and co-workers for mixtures of tetraether archaeal lipids with egg phosphatidylcholine [9].

The pure DPPC liposomes showed the characteristic phase transition at a temperature of 41 °C (Fig. 3). In the mixed liposomes, with increasing mol% $C_{25,25}$ lipids, the phase transition became less pronounced (Fig. 3). At 25 mol% $C_{25,25}$ lipids in the mixed $C_{25,25}$-DPPC liposomes the temperature of the phase transition, T_m, was 31 ± 1 °C (Fig. 3). Previously, we have reported, based on EPR measurements, that the membrane fluidity of archaeosomes of $C_{25,25}$ lipids increased with increasing temperature, although no phase transition from initial-ordered state to liquid-disordered state was detected [7]. The DPH anisotropy was higher in the pure $C_{25,25}$ lipids at temperatures higher than the T_m of DPPC of 41 °C, which means that the membrane is in more ordered form. With increase in the mol% $C_{25,25}$ lipids in the mixed $C_{25,25}$-DPPC liposomes, at temperatures above 41 °C, the order

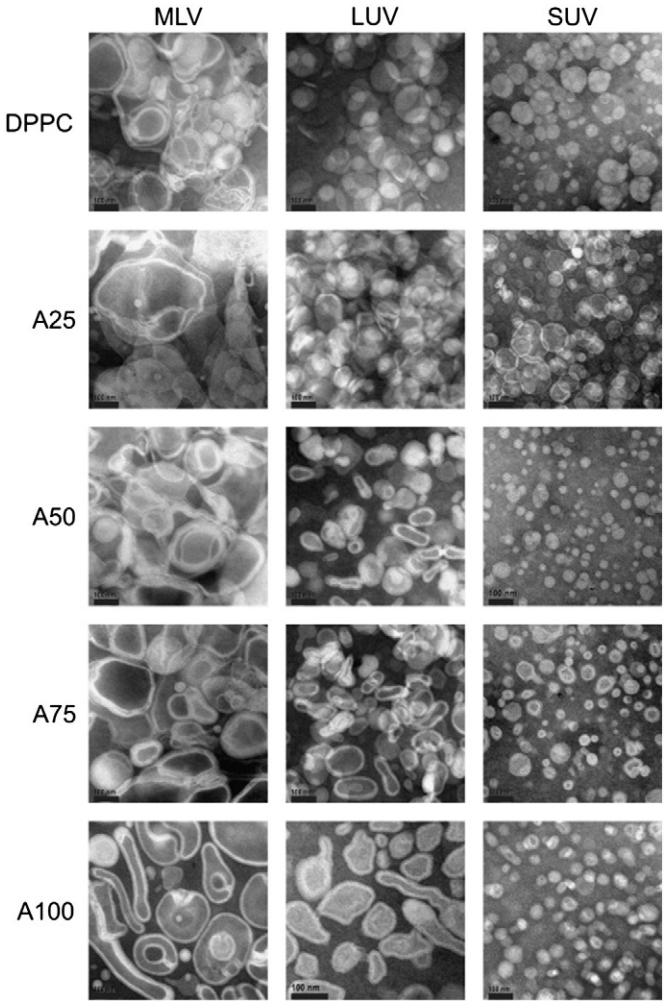

Fig. 2. TEM images of mixed $C_{25,25}$-DPPC liposomes (LUVs, SUVs, and MLVs) composed of different mol% $C_{25,25}$ lipids: 0 (DPPC), 25 (A25), 50 (A50), 75 (A75), 100 (A100) at pH 7.0.

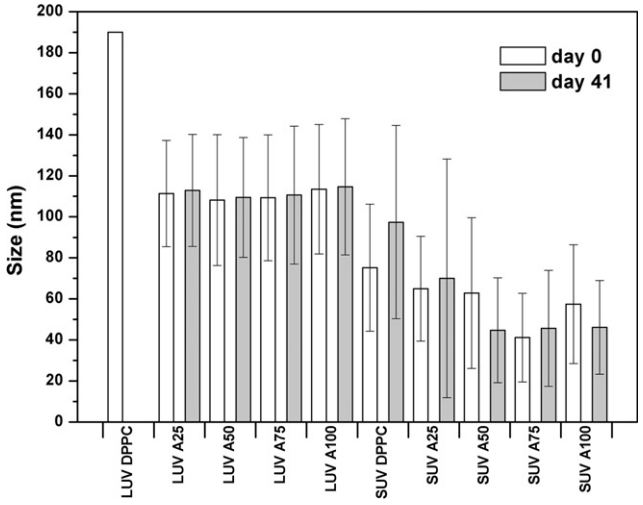

Fig. 1. Mean diameters of mixed $C_{25,25}$-DPPC LUVs and SUVs of different mol% $C_{25,25}$ lipids: 0 (DPPC), 25 (A25), 50 (A50), 75(A75), 100 (A100), measured immediately after preparation (day 0) and after 41 days.

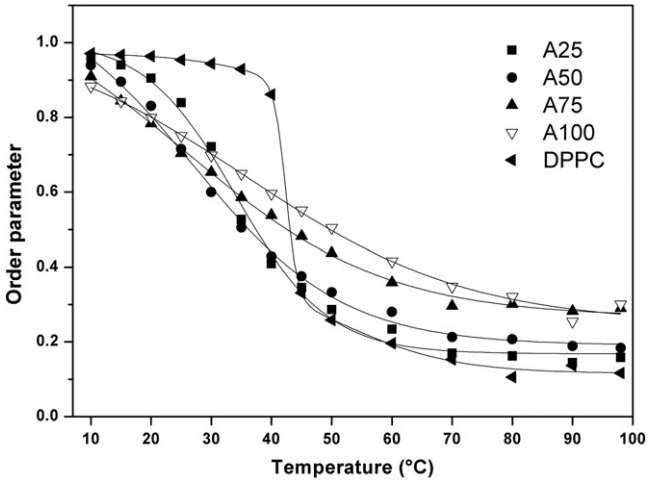

Fig. 3. Temperature-dependence of lipid order parameter (calculated from anisotropy by using Eq. (2)) of mixed $C_{25,25}$-DPPC liposomes composed of different mol%$C_{25,25}$ lipids: 0 (—DPPC), 25 (■—A25), 50 (●—A50), 75 (▲—A75), 100 (▽—A100) at pH 7.0. The solid lines represent non-linear curve fitting to the data points shown.

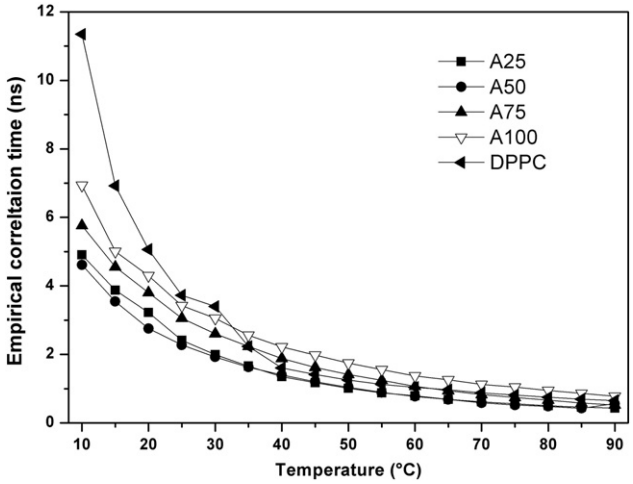

Fig. 5. Empirical correlation times of mixed $C_{25,25}$-DPPC liposomes at pH 7.0 (20 mM HEPES buffer) with different mol%$C_{25,25}$ lipids: 0 (—DPPC), 25 (■—A25), 50 (●—A50), 75 (▲—A75), 100 (▽—A100).

parameter increase (Fig. 3). Similar effects have been observed in binary lipid mixtures of DPPC with cholesterol [24], which implies that the isoprenoid alkyl chains ($C_{25,25}$) of these archaeal lipids function in the prevention of the pure lipids from forming highly ordered *gel* structures at low temperatures (below 40 °C). At higher temperatures (above 40 °C), $C_{25,25}$ prevents DPPC lipids to form completely unordered structure.

3.4. Electron paramagnetic resonance measurements

The EPR spectra of the MeFASL(10,3)-labeled mixed $C_{25,25}$-DPPC liposomes at 20 °C and pH 7.0 are shown in Fig. 4. At temperatures below 40 °C, where the DPPC liposomes were in the gel-crystalline state, all of the mixed liposomes of the $C_{25,25}$-DPPC lipids have lower empirical correlation time (τ_{emp}) than the pure DPPC liposomes, indicating that the membranes with the $C_{25,25}$ lipids were more fluid (Fig. 5). In pure DPPC vesicles, τ_{emp} at 10 °C was 11.3 ns, while in pure $C_{25,25}$ lipid vesicles τ_{emp} was 6.9 ns. However, above 40 °C (i.e. above the phase transition of DPPC), the pure $C_{25,25}$ lipid vesicles were the most rigid. In the mixed vesicles, the τ_{emp} of MeFASL(10,3) decreased with increasing concentrations of DPPC, indicating that DPPC has a fluidizing effect on the $C_{25,25}$ lipid vesicles in the interfacial parts of the membrane bilayer, throughout the whole temperature range

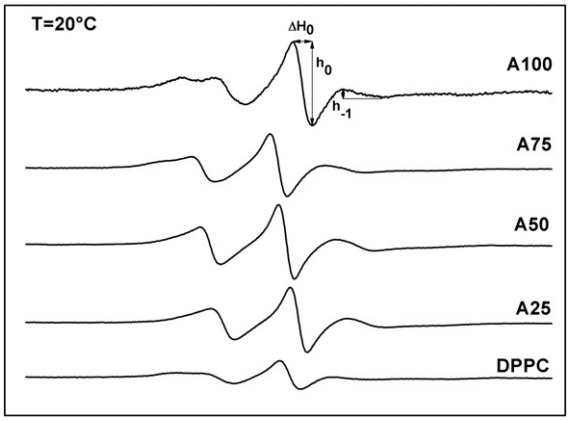

Fig. 4. EPR spectra of mixed $C_{25,25}$-DPPC liposomes at pH 7.0 (20 mM HEPES buffer) with different mol%$C_{25,25}$ lipids: 100 (A100), 75 (A75), 50 (A50), 25 (A25), 0 (DPPC) at 20 °C. In the upper spectrum, line width (ΔH_0), height of the mid-field (h_0) and height of the high-field (h_{-1}) (needed for the determination of τ_{emp}) are shown.

(Fig. 5). This is in good agreement with DPH anisotropy measurements at temperatures above 40 °C, while at temperatures where the DPPC vesicles are in the gel-crystalline phase, the results obtained with EPR were opposite to those observed by measuring DPH anisotropy. It should be stressed that DPH monitors the properties of the inner hydrophobic hydrocarbon part of the membrane, and MeFASL(10,3) monitors the the interfacial polar head group regions of the membrane [25]. Possible effect of the isoprenoid chains of the archael lipids on the doxyl moiety of the spin probe or DPH fluorophore could also be the reason for the observed differences.

In the temperature range from 10 °C to 80 °C, the τ_{emp} decreased continously with increasing temperature for all of the $C_{25,25}$-DPPC mixtures, and only in the pure DPPC condition was there a major decrease in τ_{emp}, of almost 3 ns was observed in temperature region between 30 and 45 °C. These EPR results agree well with the anisotropy data from the fluorescence spectroscopy study of DPH incorporated into these archaeosomes, and they suggest the absence of a main phase transition. Our previous DSC measurements, published elsewhere [8], confirm these conclusions.

To gain better insight into the structural characteristics of these membranes and their changes with temperature and proportion between the $C_{25,25}$ lipids and DPPC, computer simulations of the EPR spectra were performed (data not shown). In general, at temperatures below 60 °C, there was good agreement between the calculated and experimental spectra, taking into account that the spectra were the superimposition of three spectral components with different line shapes, which reflected the different modes of the spin-probe motion. This indicates that the archaeosome membranes are heterogeneous, and are composed of several regions with different fluidity characteristics. All of the regions in the membranes with the same fluidity characteristics are described by one spectral component, which represents one type of membrane nanodomain. At higher temperatures, the experimental spectra can be describe by only one spectral component, which indicates that the membranes become homogeneous, with only one domain type resolved.

The changes in the order parameters of these domain types and their proportions with temperature are shown as bubble diagrams in Fig. 6, where the dimension of each symbol (bubble) represents the population of the spin probes in the corresponding nanodomain type. The data obtained for the pure $C_{25,25}$ liposomes (Fig. 6, light gray-A100) are compared with those of pure DPPC vesicles at pH 7.0 (Fig. 6A), and with those consisting of different molar ratios of the $C_{25,25}$ lipids and DPPC (Fig. 6B–D). In Fig. 6, D1 represents the most ordered nanodomain type, with the order parameter S ~0.75 at 20 °C.

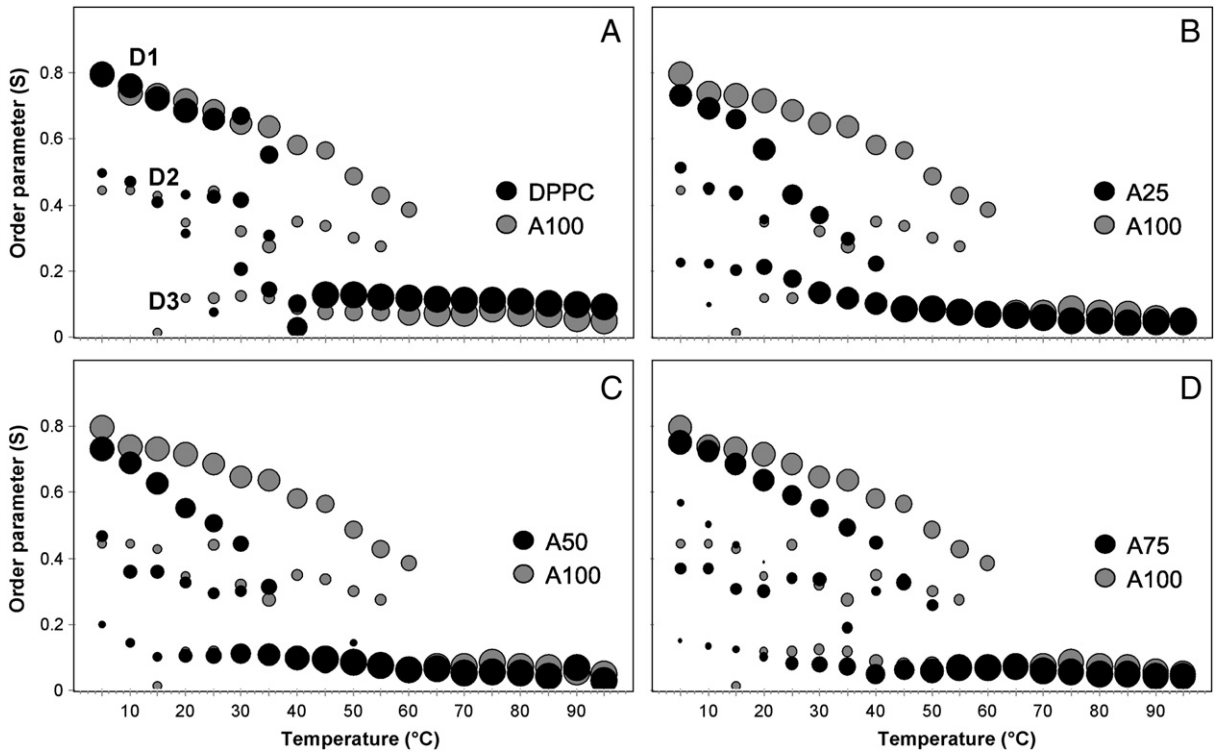

Fig. 6. Bubble diagrams of mixed $C_{25,25}$-DPPC liposomes in comparison with pure $C_{25,25}$ liposomes (A100) at pH 7.0 (20 mM HEPES buffer) at different mol%$C_{25,25}$ lipids: (A) 0 (DPPC), (B) 25 (A25) (C) 50 (A50), (D) 75 (A75).

D2 is a less-ordered nanodomain type, with S ~0.4 at 20 °C, and D3 is the least-ordered nanodomain type, with S ~0.1 across the whole temperature range measured. With increasing temperature, order parameter S and the proportion of more ordered domain types decreased, and at temperatures above 60 °C, in general, the properties of the whole membrane were reflected in one motional mode of spin probe with an order parameter S of ~0.1. The main difference between the different $C_{25,25}$-DPPC liposomes was the temperature at which the nanodomain types D1 and D2 disappeared. For pure $C_{25,25}$ lipid liposomes, D1 disappeared at 65 °C and D2 at 60 °C, while for all of the other samples, the disappearance of the most ordered component (D1) occurred at lower temperatures. The temperature at which the domains with the highest order disappeared decreased with increasing molar ratios of DPPC. The samples with 25 mol% $C_{25,25}$ lipids (A25) and in pure DPPC liposomes only one component was observed above the phase-transition temperature for DPPC. In all mixed $C_{25,25}$ lipid liposomes, the proportion of domains with a higher order decreased slowly and continuously with increasing temperature, while in the pure DPPC liposomes, there was a sudden disappearance of the D1 and D2 nanodomain types at 40 °C, which is a consequence of the phase transition from gel-to-liquid crystalline phase at this temperature; this is also reflected in the sudden decrease in τ_{emp} (Fig. 5). At the same time, with the increasing molar ratio of DPPC in the $C_{25,25}$-DPPC liposomes, the order parameter of the most ordered nanodomains decreased.

4. Conclusions

The essential general features required for the lipid membranes of extremophilic archaea to fulfill their biological functions are that they are in the liquid crystalline phase and that they also have extremely low solute permeabilities that are much less temperature sensitive due to the absence of the main gel-to-liquid crystalline phase transition and the highly branched isoprenoid chains. Significant numbers of hyperthermophilic archaea do not contain tetraether lipids [26]. The chain lengths of the C_{25}-isoprenoid hydrocarbons found in the membranes of this hyperthermophilic and neutrophilic archaea, *A. pernix,* are 20% longer than those of the C_{20}-isoprenoid and C_{18} straight-chain fatty acids [1]. Previously, we showed that the physicochemical properties of pure $C_{25,25}$ lipid liposomes (archaeosomes) do not significantly differ from those prepared from tetraether lipids [7,8].

With the aim of improving the physicochemical properties of conventional liposomes, the mixed liposomes that consisted of different types of conventional synthetic lipids and tetraether archaeal lipids were prepared and characterized [9,10]. To the best of our knowledge, there is no physicochemical data available for mixtures of diether archaeal lipids and conventional lipids such as DPPC. Based on our results presented here, it is likely that with respect to their permeability, fluidity and thermal stability, binary lipid mixtures of diether $C_{25,25}$ lipids and DPPC behave similarly as tetraether lipid and DPPC mixtures, although they are structurally different [9,10]. The model tetraether lipid membrane can be defined as an assembly of tightly packed molecules [27].

Here, we have studied the possibility of forming mixed $C_{25,25}$-DPPC liposomes, which differ in the types of bonds involved, the polar head groups, and the types and chain lengths [26]. Previously, we showed that mixed $C_{25,25}$-DPPC liposomes are characterized by very low permeabilities to calcein, even at high temperatures, and that the enthalpy and temperature of phase transition are drastically reduced with increasing the mol% $C_{25,25}$ lipids [7,8]. By increasing the mol% of these $C_{25,25}$ lipids, the permeability and the fluidity of the liposomes decreased, as can be judged from our fluorescence anisotropy and EPR measurements (Figs. 3 and 5). Discrepancies appear at temperatures below the gel-to-liquid crystalline phase transition of DPPC. Previously, we have shown by DSC that at 1:1 molar ratios of $C_{25,25}$ lipids and DPPC in mixed liposomes, the gel-to-liquid crystalline phase transition disappear [8]. TEM shows that at all molar ratios these vesicles are formed (Fig. 2), although their sizes are not very uniform, and they do not aggregate even after storage for 41 days at 4 °C (data

not shown). Photon correlation spectroscopy indicated that the vesicle diameters in the mixed $C_{25,25}$-DPPC liposomes containing ≥50 mol% $C_{25,25}$ lipids did not change. At lower mol% (higher contents of DPPC), the diameters of the resultant vesicles were greater, which can also be seen from TEM images. The vesicles made of pure $C_{25,25}$ lipids have more defined structures (Fig. 2). After 41 days, the sizes of the pure DPPC liposomes increased, while the sizes of the mixed $C_{25,25}$-DPPC vesicles (MLVs and SUVs) did not change significantly (Fig. 1). These results indicate that the mixed $C_{25,25}$-DPPC liposomes do not fuse or aggregate after storage for 41 days at 4 °C. Similar results have been obtained for tetraether archaeal lipids [4,28].

Acknowledgements

The authors would like to express their gratitude for financial support from the Slovenian Research Agency through Research Program P4-0121 and Project J2-3639.

References

[1] H. Morii, H. Yagi, H. Akutsu, N. Nomura, Y. Sako, Y. Koga, A novel phosphoglycolipid archaetidyl(glucosyl)inositol with two sesterterpanyl chains from the aerobic hyperthermophilic archaeon *Aeropyrum pernix* K1, Biochimica et Biophysica Acta, Molecular and Cell Biology of Lipids 1436 (1999) 426–436.
[2] M. Derosa, A. Gambacorta, A. Trincone, A. Basso, W. Zillig, I. Holz, I, Lipids of thermococcus-celer, a sulfur-reducing archaebacterium—structure and biosynthesis, Systematic and Applied Microbiology 9 (1987) 1–5.
[3] A. Gambacorta, A. Gliozzi, M. Rosa, Archaeal lipids and their biotechnological applications, World Journal of Microbiology and Biotechnology 11 (1995) 115–131.
[4] D.A. Brown, B. Venegas, P.H. Cooke, V. English, P.L.G. Chong, Bipolar tetraether archaeosomes exhibit unusual stability against autoclaving as studied by dynamic light scattering and electron microscopy, Chemistry and Physics of Lipids 159 (2009) 95–103.
[5] P.L.G. Chong, Archaebacterial bipolar tetraether lipids: physico-chemical and membrane properties, Chemistry and Physics of Lipids 163 (2010) 253–265.
[6] N.P. Ulrih, U. Adamlje, M. Nemec, M. Sentjurc, Temperature- and pH-induced structural changes in the membrane of the hyperthermophilic archaeon *Aeropyrum pernix* K1, Journal of Membrane Biology 219 (2007) 1–8.
[7] D. Gmajner, A. Ota, M. Sentjurc, N.P. Ulrih, Stability of diether C25,25 liposomes from the hyperthermophilic archaeon *Aeropyrum pernix* K1, Chemistry and Physics of Lipids 164 (2011) 236–245.
[8] D. Gmajner, N.P. Ulrih, Thermotropic phase behaviour of mixed liposomes of archaeal diether and conventional diester lipids, Journal of Thermal Analysis and Calorimetry (2011), doi:10.1007/s10973-011-1596-4.
[9] P.I. Lelkes, D. Goldenberg, A. Gliozzi, M. Derosa, A. Gambacorta, I.R. Miller, Vesicles from mixtures of bipolar archaebacterial lipids with egg phosphatidylcholine, Biochimica et Biophysica Acta 732 (1983) 714–718.
[10] Q. Fan, A. Relini, D. Cassinadri, A. Gamba`corta, A. Gliozzi, Stability against temperature and external agents of vesicles composed of archaeal bolaform lipids and egg PC, Biochimica et Biophysica Acta (BBA)—Biomembranes 1240 (1995) 83–88.
[11] R. Sasaki, H. Sasaki, S. Fukuzawa, J. Kikuchi, H. Hirota, K. Tachibana, Thermal analyses of phospholipid mixtures by differential scanning calorimetry and effect of doping with a bolaform amphiphile, Bulletin of the Chemical Society of Japan 80 (2007) 1208–1216.
[12] D.P. Brownholland, G.S. Longo, A.V. Struts, M.J. Justice, I. Szleifer, H.I. Petrache, M.F. Brown, D.H. Thompson, Phase separation in binary mixtures of bipolar and monopolar lipid dispersions revealed by 2H NMR spectroscopy, small angle X-ray scattering, and molecular theory, Biophysical Journal 97 (2009) 2700–2709.
[13] P.L.-G. Chong, R. Ravindra, M. Khurana, V. English, R. Winter, Pressure perturbation and differential scanning calorimetry of bipolar tetraether liposomes derived from the thermoacidophilic archaeon *Sulfolobus acidocaldarius*, Biophysical Journal 89 (2005) 1841–1849.
[14] I. Milek, B. Cigic, M. Skrt, G. Kaletunc, N.P. Ulrih, Optimization of growth for the hyperthermophilic archaeon *Aeropyrum pernix* on a small-batch scale, Canadian Journal of Microbiology 51 (2005) 805–809.
[15] E.G. Bligh, W.J. Dyer, A rapid method of total lipid extraction and purification, Canadian journal of biochemistry and physiology 37 (1959) 911–917.
[16] H. Pottel, W. van der Meer, W. Herreman, Correlation between the order parameter and the steady-state fluorescence anisotropy of 1,6-diphenyl-1,3,5-hexatriene and an evaluation of membrane fluidity, Biochimica et Biophysica Acta (BBA)—Biomembranes 730 (1983) 181–186.
[17] L. Coderch, J. Fonollosa, J. Estelrich, A. De La Maza, J.L. Parra, Influence of cholesterol on liposome fluidity by EPR—relationship with percutaneous absorption, Journal of Controlled Release 68 (2000) 85–95.
[18] J. Strancar, M. Sentjurc, M. Schara, Fast and accurate characterization of biological membranes by EPR spectral simulations of nitroxides, Journal of Magnetic Resonance 142 (2000) 254–265.
[19] Z. Arsov, J. Strancar, Determination of partition coefficient of spin probe between different lipid membrane phases, Journal of Chemical Information and Modeling 45 (2005) 1662–1671.
[20] M.E. Johnson, D.A. Berk, D. Blankschtein, D.E. Golan, R.K. Jain, R.S. Langer, Lateral diffusion of small compounds in human stratum corneum and model lipid bilayer systems, Biophysical Journal 71 (1996) 2656–2668.
[21] J. Strancar, T. Koklic, Z. Arsov, Soft picture of lateral heterogeneity in biomembranes, Journal of Membrane Biology 196 (2003) 135–146.
[22] J. Strancar, T. Koklic, Z. Arsov, B. Filipic, D. Stopar, M.A. Hemminga, Spin label EPR-based characterization of biosystem complexity, Journal of Chemical Information and Modeling 45 (2005) 394–406.
[23] X.L. Xu, E. London, The effect of sterol structure on membrane lipid domains reveals how cholesterol can induce lipid domain formation, Biochemistry 39 (2000) 843–849.
[24] P.L. Chong, D. Choate, Calorimetric studies of the effects of cholesterol on the phase transition of C(18):C(10) phosphatidylcholine, Biophysical Journal 55 (1989) 551–556.
[25] V. Noethig-Laslo, M. Sentjurc, A.L. Liu, Advances in planar lipid bilayers and liposomes, in: A.L. Liu (Ed.), Transmembrane Polarity Profile of Lipid Membranes, vol. 5, Academic Press, Amsterdam, 2006, p. 50.
[26] N.P. Ulrih, D. Gmajner, P. Raspor, Structural and physicochemical properties of polar lipids from thermophilic archaea, Applied Microbiology and Biotechnology 84 (2009) 249–260.
[27] J. Nicolas, A molecular dynamics study of an archaeal tetraether lipid membrane: comparison with a dipalmitoylphosphatidylcholine lipid bilayer, Lipids 40 (2005) 1023–1030.
[28] C.G. Choquet, G.B. Patel, G.D. Sprott, Heat sterilization of archaeal liposomes, Canadian Journal of Microbiology 42 (1996) 183–186.